Classification of Dynamical Vertical Climbing Gaits

Jason M. Brown, Bruce D. Miller, and Jonathan E. Clark

***Abstract*— While numerous gaits in the horizontal regime (e.g. walking or running) have been defined for legged systems on level ground, no dynamically grounded definitions have been developed for dynamic vertical running. Gaits have clear implications to robotic control strategy, efficiency, and stability. However, while several climbing robotic systems have been described as achieving 'running', the question of whether distinct dynamic gaits exist and what classifies these gaits has not been rigorously explored. In this paper, by applying definitions developed in the horizontal regime, we show evidence of three distinct gaits as well as discuss the implications of these gaits on the development of dynamic climbing systems.**

I. Introduction

For legged locomotion on level ground, dynamic gaits are often classified as 'walking' or 'running.' While the difference between these can often be qualitatively identified through visual observation (such as the presence of a flight phase), more quantitatively grounded metrics can be (and often are) used as well, including shape factor [1], Froude number [1], and phasing between kinetic energy and gravitational potential energy [9]. Historically, fundamentally different models (ballistic motion for dynamic walking [17] [10] [20] and Spring Loaded Inverted Pendulum (SLIP) for running [3] [4]) have been used to explain, analyze, and develop reliable controllers and robust robotic systems. Dynamic gaits have implications for more than just speed, as the control approaches as well as the associated stability and efficiency are greatly impacted by the gait chosen.

Numerous robotic platforms have been built that are capable of instantiating these gait families. Quasi-static walkers, such as ASIMO [22], leverage complex control strategies to stand and move, allowing for the implementation of varied and complex tasks, but with limited locomotion efficiency. Another approach has been to embed the passive dynamics of the models into system design, such as passive dynamic walkers [6] which utilize ballistic motion and running platforms [21] [23] which instantiate SLIP dynamics, which result in systems that are efficient and robust to perturbations, while requiring minimal control effort.

Similar to their horizontal counterparts, climbing platforms have also been developed which utilize quasi-static locomotion and other, dynamic, platforms based on spring mass models. Much of the earliest success was seen in quasi-static platforms [13], [14], [24], some of which are flexible enough to climb non-planar, real world surfaces [15], but have not been able to approach the locomotive speeds seen in their biological counterparts, such as geckos [2], on any surface. To approach these velocities, dynamic climbing platforms, such as BOB (see Fig 1a) have been developed embedding the dynamics of the Full-Goldman (FG) model [12], which captures the planar yaw dynamics of geckos and cockroaches running up walls.

Department of Mechanical Engineering, Florida State University, Tallahassee, FL, 32310 USA e-mail: jmb10t@my.fsu.edu.

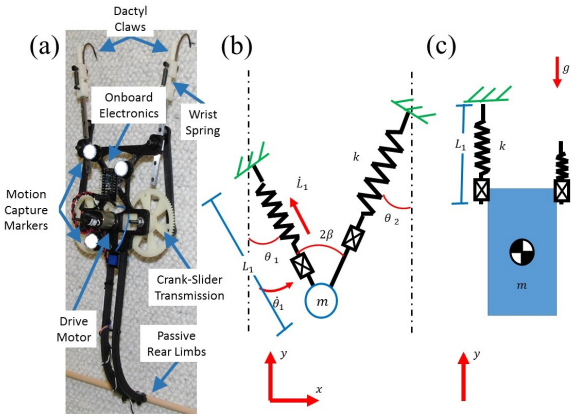

Fig. 1: (a) Picture of the miniature bipedal dynamic climbing platform called BOB. A single actuator at the center of the platform drives both gears, which are physically locked 180° out of phase to move the linear guide rails. (b) Simplified Full-Goldman Template which BOB based on with two springy legs at a fixed angular offset. (c) 1D dynamic climbing template removing angular offset and restricting motion strictly vertical.

While extensive study has been focused on characterizing gaits for level-ground locomotion, little rigor has been applied to dynamic climbing and we often simply describe rapid vertical travel as 'running' without applying any quantitative metrics to support this statement.

More recent modeling work [11] has shown that in the horizontal domain both dynamic walking and running behaviors can be exhibited by a simple bipedal spring-leg model. This, in turn, has led to design and control strategies [7] for building robots that can utilize both dynamic regimes.

Inspired by this, we examine if and how different gaits can emerge from a simplified Full-Goldman-based dynamic climbing template [12] and what the characteristics of these gaits are. We demonstrate for the first time the clear presence of distinct 'walking' and multiple running regimes in this dynamic climbing model. Additionally, we discuss the differences in these climbing modalities with respect to horizontal domain standards and address the implications of these findings on the design and control of climbing robots.

II. Modeling

A. Full-Goldman (FG) Template

The FG template was developed after observing similarities in locomotion dynamics of cockroaches and geckos rapidly scaling vertical surfaces. While these animals have distinctly different morphologies and footfall patterns, the ground reaction force and velocity profiles were qualitatively similar. The template captures these patterns with a simple model consisting of a point mass body and springy legs.

This model has served as a template for a series of dynamic climbing platforms. The first of these was Dyno-Climber [16], which is currently the fastest legged climbing robot. Later, a simplified dynamically scaled version of Dyno-Climber called BOB was developed [8] (Fig. 1a). The latest iteration is SCARAB, which demonstrated FG based climbing in a quadruped [19].

B. Reduced Order Modeling

The FG model BOB is based on is shown in Fig. 1b, which consists of two linearly-actuated, springy limbs attached to a point mass body at a fixed angular offset, where attachment points are treated as pin joints while engaged. The system climbs by contracting the attached leg, which with the angular offset causes the body to rotate and the spring to stretch and retract, while extending the unattached leg until the next attachment point is reached, causing the previously attached leg to detach and the cycle to repeat.

To isolate the vertical and rotational dynamics of the system, a 1D version of the simulation shown in Fig. 1c, similar to the formulation in [5], was created by setting the fixed angular offset to zero and having no angular perturbations. The 1D system still has a point mass, but the system starts perfectly vertical and attachment is now treated as a rigid joint.

A difference between the models discussed in this paper and previously studies is the adaptation of an attachment scheme which uses a state-based attachment approach (i.e., directional adhesion) rather than a timing-based protocol. This results in a more realistic model of attachment/detachment based on the force in the leg.

C. Equations of Motion (EOMs)

The EOMs were determined using Newton's method in the global Cartesian coordinate frame as the reference frame. The Cartesian frame was chosen for the two dimensional model to simplify the transitions between states. Both models utilize (1) and (2); however, the one dimensional model starts with $\theta_1 = \theta_2 = 0$, which reduces the motion to the vertical direction. The actuation scheme uses a sinusoidal trajectory, (3), based on the physical platform and actuation model used in previous studies [16] which fixes the limbs at 180° out of phase.

Using Cartesian coordinates for the two dimensional model sets the state variables as X, Y instead of L, θ, but L and θ are still required to compute the forces in the springs. The spring force is necessary for both the EOMs and the switching conditions discussed below. Thus the foot position is tracked and used to determine the actual leg length at each instant. With knowledge of the foot position, the leg length and angle can be calculated using (4) and (5).

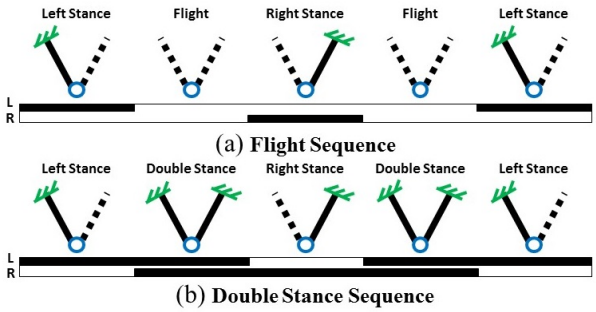

(a) **Flight Sequence**

(b) **Double Stance Sequence**

Fig. 2: (a) Shows the phase changes which occurs for gaits with a flight phase. The system starts with a single attachment then completely detaches from the surface before the second limb attaches. (b) Shows the phase changes which occur for gaits with a double support phase. The system starts in single support, then the second limb attaches before the first limb has reached the conditions for detachment.

$$\ddot{X} = -\frac{Leg_1}{m}k(L_1 - L_{mtr_1})\sin(\theta_1) - \frac{Leg_2}{m}k(L_2 - L_{mtr_2})\sin(\theta_2) \tag{1}$$

$$\ddot{Y} = -g + \frac{Leg_1}{m}k(L_1 - L_{mtr_1})\cos(\theta_1) + \frac{Leg_2}{m}k(L_2 - L_{mtr_2})\cos(\theta_2) \tag{2}$$

$$L_{mtr_i} = L_{nom} + \frac{L_{stroke}}{2}\cos(2\pi\Omega t) \tag{3}$$

$$L_i = \sqrt{(X_{foot_i} - X)^2 + (Y_{foot_i} - Y)^2} \tag{4}$$

$$\theta_i = \arctan\frac{X_{foot_i} - X}{Y_{foot_i} - Y} \tag{5}$$

D. Switching Conditions

The threshold for the foot to either engage or detach from the substrate is formulated as follows. During stance, each foot remains engaged as long as the force in the leg remains in tension:

$$F_{leg} > 0. \tag{6}$$

This can be calculated directly in the simulation by the sum of the spring (and damper) forces in the leg:

$$F_k + F_b = k\Delta L + b\dot{L} > 0. \tag{7}$$

To determine when the foot engages with the substrate during flight, we consider the motion of the foot along the substrate along the axis of the leg (i.e. directional adhesion):

$$V_f < 0, \tag{8}$$

TABLE I: Parameter settings for climbing sweeps.

Parameter	Description	Value
g	Gravitational Constant	9.81 ms^{-2}
Leg_i	Flag for Attachment of Leg i	[0 or 1]
L_{nom}	Nominal Length of Leg	0.2 m
L_{stroke}	Stroke Length of Leg	0.05 m
k	Spring Stiffness of Arm Spring	130 Nm^{-1}
β	Sprawl Angle	20 deg
b	Damping Ratio	0 N s m^{-1}
m	Body Mass	0.3 kg
Ω	Driving Frequency	1-6 Hz

where V_f is the velocity of the foot in the direction of the leg in the global frame, which can be determined as:

$$V_f = \dot{X}\sin(\theta+\beta)+\dot{Y}\cos(\theta+\beta)+\dot{L}, \tag{9}$$

where $\dot{X}$ and $\dot{Y}$ are the horizontal and vertical velocity of the body, respectively, θ is the body angle, β is the sprawl angle, and $\dot{L}$ is the rate of extension(+)/retraction(-) of the leg as dictated by the controller.

Since this model simulates directional adhesion unlike previous FG analysis, the system can follow several different flow patterns which include flight with no limbs attached to a surface and double support where both limbs are attached to the surface. For this paper, the sequence of flows that will be considered are shown in Fig. 2 and the boundary case, where there are only single support phases.

E. System Parameters

The simulation was run with the physical parameters of the current version of BOB, tabulated in Table I. The parameters for BOB were chosen to allow for direct comparison with experimental data and to give reference for achievable driving frequencies. While a direct comparison to the robot will be considered in future work, the goal here is to identify and understand the fundamentals of the gait dynamics and as such, no damping was added to the system.

III. Simulation Results

For the range of values given in Table I, Newton-Raphson fixed point searches were implemented to determine steady state behavior of the system. Once fixed points were determined, efficiency, ground reaction forces, climbing velocity, duty factor, stroke length, and the phasing between kinetic energy and gravitational potential energy were determined. Efficiency was determined using the cost of transport definition $CoT = \frac{E_{in}}{E_{Out}}$ where $E_{in} = Leg_1(k(L_1 - L_{mtr_1}))\dot{L}_{mtr_1} + Leg_2(k(L_2 - L_{mtr_2}))\dot{L}_{mtr_2}$ and $E_{out} = mg(\Delta h)$. The phasing between kinetic energy and gravitational potential energy is computed using the definition given by Full and Tu [9].

A. Identification of Distinct Trajectories

For running on level ground, the simplest method of identifying possible gaits is the transition from the presence of a double support phase to gaits which experience flight. Fig. 3 shows the COM trajectories for the 1D and 2D models

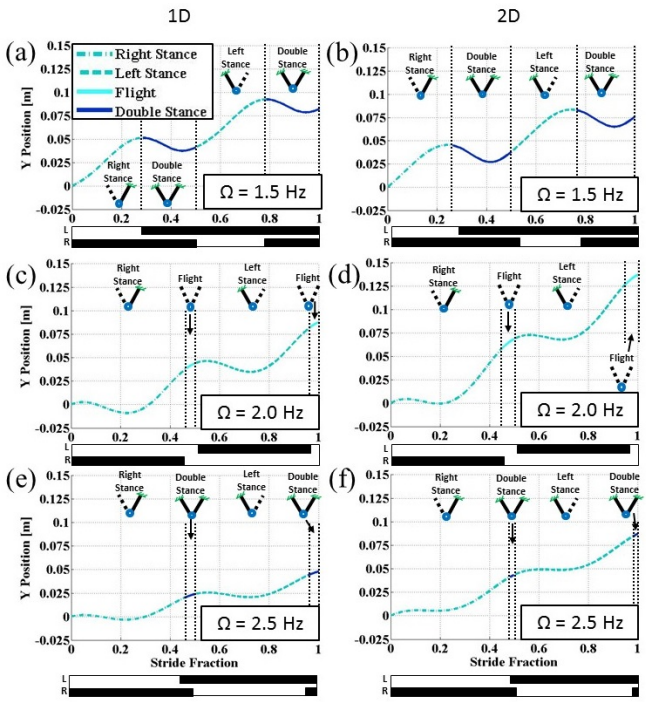

Fig. 3: Set of trajectories from both the 1D (shown on the left) and 2D (shown on the right) simulation at discrete frequencies. The top row, (a) and (b) shows the simulation at 1.5 Hz which results in a double stance flow. Increasing the frequency to 2.0 Hz, (c) and (d) results in a flight flow. Then, running the simulation at 2.5 Hz, (e) and (f) results in a double stance flow.

at driving frequencies (Ω) of 1.5 Hz, 2.0 Hz and 2.5 Hz. To directly compare the 1D and 2D trajectories as well as show that distinct footfall patterns exist, the vertical position of the COM vs stride percentage are shown with the current phase highlighted.

Examining the trajectories at the same driving frequency shows the 1D and 2D simulations are qualitatively similar. The footfall patterns in Fig. 3a,b,e, and f all have a double stance phase, while the trajectories in Fig. 3c and d have a flight phase. The first set of trajectories, shown in Fig. 3a and b, start gaining vertical position while in single stance, then transition to double stance and lose vertical position only to gain further vertical position in the next single stance phase. The second set of trajectories, shown in Fig. 3c and d, lose vertical position while in the first half of a single stance phase then begin gaining height during the second half of stance, which continues until flight occurs. A momentary peak occurs at the beginning of the next stance phase and the cycle continues. The third type of trajectory, shown in Fig. 3e and f, has a similar pattern as Fig. 3c and d, but instead of experiencing flight, the system experiences double stance while continuing to rise. Additionally, the higher frequency gait has a shorter stroke length than the intermediate frequency gait as seen from the total height gained over the course of a stride.

An examination of Fig. 3 shows three distinct families of trajectories. At low frequencies, double stance gaits arise with the loading of the legs springs occurring during double stance. At intermediate frequencies, flight phases exist with loading occurring during single support. At higher frequencies, double stance gaits exist with loading occurring during single support. This suggests there are at least three different gait behaviors that can be exhibited by dynamically climbing systems, however, the presence of double stance gaits at driving frequencies higher than the flight gaits suggests that duty factor and COM motion are not sufficient to fully characterize and classify these gaits.

B. Classification of Gaits

In order to understand and classify these gait patterns we employ additional, quantitative definitions of gaits. The first definition considered involves the shape of the ground reaction force profiles. In the horizontal regime, dynamic walking gaits have ground reaction force profiles over the course of a step which have a symmetric double peak, while running gaits have a single peak during the course of a step [1]. The second definition utilized will be the relative phasing of the peak kinetic energy and gravitational potential energy. In horizontal locomotion, the kinetic and gravitational potential energy are in phase for running gaits, and are 180 degrees out of phase for walking gaits [9].

1) Ground Reaction Force Comparison: The ground reaction force profiles for each of the trajectories described previously are shown in Fig. 4. As with the vertical trajectories, the qualitative behavior of the 1D and 2D systems were the same. However, the magnitudes of the vertical ground reaction forces are consistently higher for the 2D model, which can be explained by the increased energy stored in the system from the pendular motion which increases the load on the feet.

The gait at 1.5 Hz, the lowest driving frequency shown, has a ground reaction force pattern, shown in Fig. 4a and b over the course of a stride, that has 2 peaks over the course of a step. For this gait, the highest total ground reaction force occurs during a double stance phase. The gait at 2.0 Hz has a ground reaction force pattern, shown in Fig. 4c and d, which only has a single peak over the course of a step. While the gait at 2.5 Hz has no flight phase and has a double stance phase, it also has a single peak in the ground reaction force pattern, shown in Fig. 4e and f.

The low frequencies gaits, including $\Omega = 1.5\,\text{Hz}$, appear to correspond to dynamic walking in the horizontal domain, which occurs at lower driving frequencies, have a double support phase, and the loading for the next step occurs during double support phases. The moderate frequency gaits, including $\Omega = 2.0\,\text{Hz}$, correspond to a running gait in the horizontal domain. This gait meets the standard definition of running, since it has a flight phase, it occurs at a higher driving frequency than the previously defined walking, and it has a single peak in the ground reaction force pattern. The higher frequency gaits, including $\Omega = 2.5\,\text{Hz}$, have a single peak which suggests that these are running gaits, but the

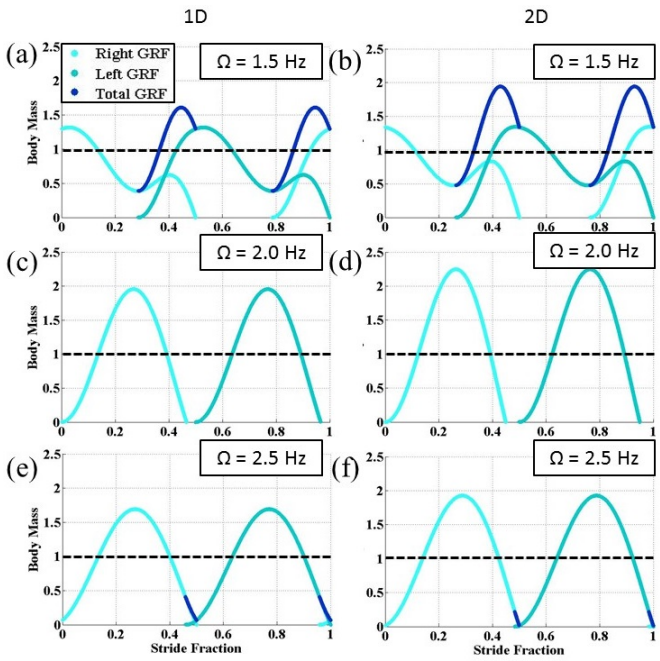

Fig. 4: Set of ground reaction force profiles from both the 1D (shown on the left) and 2D (shown on the right) simulation at discrete frequencies. The top row, (a) and (b) shows the simulation at 1.5 Hz which results in a profile with a double peak. Increasing the frequency to 2.0 Hz, (c) and (d) results in a single. Then, running the simulation at 2.5 Hz, (e) and (f) also results in a single peak, but has a double support phase.

double stance phase is uncommon for bipedal running. The only way a horizontal system experiences this type of gait behavior is in compliant or Groucho running [18].

2) Energy Phasing: The second metric that we examine is the phasing between the peak gravitational potential energy and kinetic energy. Since a climbing system gains gravitational potential energy over the course of a step, the phasing was calculated by examining the variation from the average increase in gravitational potential energy. The results, shown in Fig. 5, show a clear difference between the dynamic walking gaits and running gaits in the 2D system, where the dynamic walking gaits' peak kinetic energy leads the gravitational potential energy by about 120° while in the running gaits the kinetic energy lags behind the potential energy by about 60°.

Within the horizontal domain, dynamic walking gaits are defined by the kinetic energy and the potential energy being 180° out of phase while running gaits are in phase. Within the climbing regime, there is also a 180° phase difference, but the phase is shifted 60°.

Consideration of the energy phasing confirms our observations from the ground reaction forces and COM trajectories that dynamic climbing can be classified into 3 distinct gaits. At low frequencies there is a dynamic walking gait with a double hump ground reaction force profile and phasing between kinetic energy and gravitational potential energy

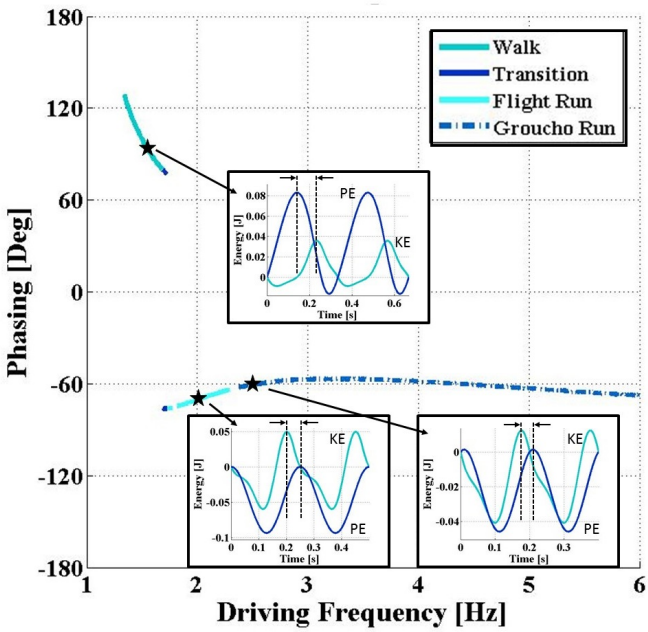

Fig. 5: The phasing difference between the kinetic energy and gravitational potential energy for the 2D model for a frequency range from 1-6 Hz. The phasing profiles of the gaits shown previous are also shown and a clear phase shift can be seen, as the walking gait is almost out of phase while the running gaits are almost in phase.

close to 180° out of phase. At moderate frequencies, climbing results in running gaits, with the presence of a flight phase, a single peak in the ground reaction force profile and the kinetic energy and gravitational potential energy being close to in phase. At higher frequencies, gaits are also clearly running based on the ground reaction forces and the phasing between kinetic energy and gravitational potential energy, but the short stroke lengths produce small steps with double support phases resembling Groucho [18], or compliant, running.

Furthermore, Fig. 5 shows the ranges of stride frequencies that result in each of the 3 gaits. The transition between dynamic walking and flight running is identifiable from the phase shift, and flight running becomes Groucho running when the duty factor equals 0.5, shown by the dashed line on Fig. 6b.

IV. Discussion

By examining and directly comparing the trajectories from the 1D model, which is regulated by spring mass dynamics, and the 2D model, which is governed by both the spring mass dynamics and pendular dynamics, the mechanism for gait dynamics can be determined. While there are some quantitative differences, the qualitative similarity indicates that the gait behavior is defined primarily by the spring mass system rather than the pendulum dynamics of the 2D system. With this in mind, we will utilize the 1D simulation to compare the climbing gaits to their level-ground running counterpart, examine gait transitions, and discuss gait selection criteria.

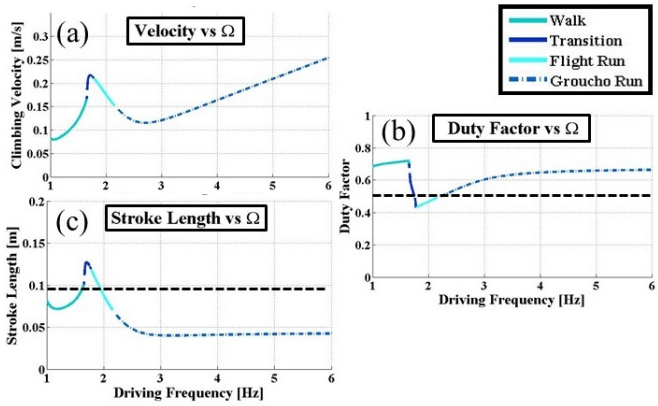

Fig. 6: Several standard classifications for the horizontal regime applied to vertical domain for the 1D simulation over a range of driving frequencies. (a) shows the relation of climbing velocity to driving frequency, (b) shows the duty factor vs driving frequency, and (c) shows the stroke length vs driving frequency.

These results were then confirmed with the 2D model but not shown for brevity.

A. Characterization with respect to Horizontal Domain

Having determined that three unique gaits exist using horizontal domain definitions of dynamic walking and running, the next step is to classify the performance of each gait and how they differ from their horizontal domain counterpart. The first difference can be seen in the relationship between for-aft velocity and stride frequency, shown in Fig. 6a. For most animals including geckos and cockroaches, this is a monotonic relation [9]. The simulation, however, has a local maximum in climbing velocity which occurs in the flight gaits shortly after the walk to run transition, then decreased with increasing driving frequency. This decrease continues into the initial compliant running gaits, reaches a local minimum and then increases in an almost linear fashion.

Comparing the climbing velocity behavior, Fig. 6a, with the stroke length behavior, Fig. 6c, helps explain this peak and highlights another difference between the horizontal and vertical regimes. The peak for climbing velocity corresponds to a peak in the stroke length, which is a departure from the horizontal regime where the stroke length continues to increase with driving frequency [1]. After this peak, the stroke length decreases but eventually settles to a value which is almost independent of driving frequency. Once the system settles to this stroke length, the velocity increases almost linearly.

The duty factor profile also deviates since the duty factor increases with increasing driving frequency after the transition from walking to running. This difference, which will be discussed more later, could be a major factor in choosing which gait to employ. Having a duty factor above 0.5 ensures that the climbing system remains attached to the surface with at least one foot at all times. Since achieving and maintaining attachment is one of the primary concerns in

climbing, keeping a secure foot attached reduces the chance of catastrophic failure.

B. Mechanism for Walk to Run Transition

Having determined the driving frequencies at which walking and running occur, the transition between these gaits can be explored. Fixed point searches in the 2D system find a region where both fixed points for dynamic walking and flight running gaits exist, similar to what is seen in the horizontal domain [1].

As the stride frequency increases within the walking region and approaches the transition to running, the system's stroke length approaches the actuator stroke length, shown by the dashed line on Fig. 6c. Once the stroke length exceeds the limit of the actuator stroke length, flight phases occur.

The transition from flight running to Groucho running occurs for the opposite reason. At high enough frequencies, the body velocity does not stay above the actuator velocity. Eventually, the second limb touches down before the first limb lifts off, which causes the stroke length to be shortened and the climbing velocity to be reduced.

C. Model Parameter Variation

While only the results with parameters from BOB have been presented, additional 1D simulations were run with a range of spring stiffnesses. The results have the same transitions and qualitative behavior, but the transition points shift. For stiffer systems, the peak ground reaction forces decrease with increasing frequency and the duty factor increases with increasing driving frequency. For very stiff systems ($k > 200$) compliant running does not appear in the frequency range tested.

D. Gait Selection

Having shown the existence of three unique gaits and compared these gaits with horizontal regime trends, the question can then be asked: when should a specific gait be used? As previously mentioned, attachment is one of the limiting factors to dynamic climbing robots where the limit is either the strength of the surface or the strength of the interface between robot and the surface. Therefore limiting the peak ground reaction force is desirable for climbing. The peak ground reaction forces vs driving frequency seen in Fig. 7a show that the highest ground reaction forces occur during flight running. The peak ground reaction force then decreases with increasing frequency for Groucho running gaits.

While the Groucho running has the lowest peak ground reaction force for running, dynamic walking gaits have lower ground reaction forces still. This could be important for larger systems, as attachment limits are challenging to scale. Current attachment technology can be scaled to increase the surface area of attachment, but the surface strength is only dependent on the material properties which do not change with size.

Often, the goal is to maximize climbing velocity within the constraints of real systems. Fig. 7b shows that several

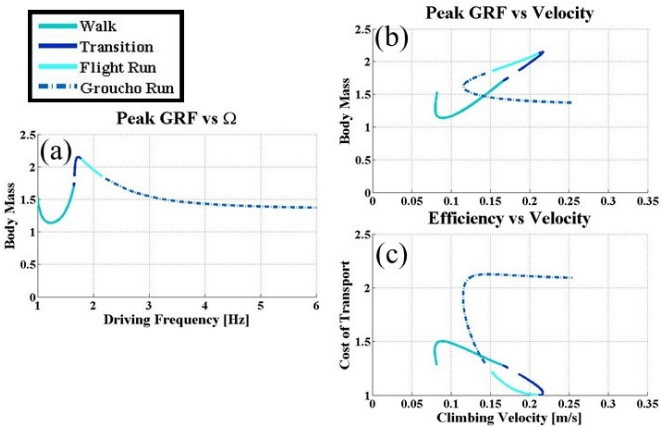

Fig. 7: Some implications of the difference between the horizontal domain and vertical domain are the need to reduce the peak ground reaction force. (a) shows the peak ground reaction force vs driving frequency to show the identify the behavior for the different gaits. (b) shows the peak ground reaction force vs climbing velocity which is not monotonic so several gaits produce the same climbing velocity. (c) shows the efficiency for choosing gaits with a lower ground reaction force.

gaits can achieve the same speed, but have different peak ground reaction forces. Fig. 7b shows there is a clear overlap between the dynamic walking and Groucho running gaits, which suggest that for max climbing velocity you would want to use a dynamic walking gait with a driving frequency below 1.6 Hz and then jump and use the higher frequency Groucho running gaits at a driving frequency above 3.5 Hz. This is a significant deviation from standard practices which would sweep continuously through a range of driving frequencies.

While compliant running limits the peak ground reaction force, it does not maximize efficiency as seen in Fig. 7c. For climbing, since the system is continually gaining energy, the theoretical optimal COT is 1 where all energy input into the system results in an increase in the systems' gravitational potential energy. The flight running gaits achieve this limit since the simulation was run without any damping and the only losses come from the additional energy required to drive the system in double stance. For compliant running, the system settles to an efficiency of approximately 2, requiring twice as much energy input during the course of a stride to climb the same distance as the optimal flight gait.

While the peak ground reaction force is a limiting factor as a system increases in mass, an additional factor in climbing success is the ability to recover from attachment failure. For the compliant running gaits, if the next attachment fails, there is still a foot in contact on an attachment point which has already supported the peak ground reaction force. However, for the flight running gaits, there is no foot in contact when a new foot attaches, and if the next foothold fails, the system may catastrophically fail. However, a lighter platform, which produces smaller ground reaction forces, combined with an

actuation scheme that ensures attachment could utilize flight gaits which are significantly more efficient and faster than comparable Groucho running gaits.

V. Conclusion and Future Work

In this paper, we show evidence of 3 distinct dynamic gaits for vertical motion: dynamic walking gaits, flight running gaits and compliant running gaits. Those gaits are identified and classified using definitions from the horizontal domain including the shape of ground reaction force profiles and phasing between peak kinetic energy and gravitational potential energy. We show that essentially the same gait behavior occurs in both the 1D and 2D models suggesting that gaits transitions are governed by the spring mass dynamics inherent in the 1D model.

The climbing system shows both gaits with flight and double stance gaits, but double stance gaits appear at both low driving frequencies and high driving frequencies. This led to the identification of compliant or Groucho running as a climbing modality, and that these running gaits minimize the peak ground reaction force, a key characteristic for improved surface adhesion. Flight gaits appear at intermediate driving frequencies, which is unlike the horizontal domain where flight running occurs for all frequencies above walking. Flight gaits are faster and more efficient than compliant running gaits, but may not be reliable and safe for current climbing systems.

Thus to maximize velocity while minimizing peak ground reaction force, a discontinuous set of driving frequencies should be used. For the system with BOB parameters, this translated to using the dynamic walking gaits at frequencies below 1.6 Hz and then jumping to 3.5 Hz or above to compliant running gaits.

Future investigations can extend the current work by exploring these gaits with physical limitations of real world systems. The first extension is to explore gait dynamics in simulations which include damping and motor limits, allowing for more direct comparison with existing experimental platforms. The second extension is to experimentally validate the existence of distinct gaits in climbing by showing these trajectories and ground reaction force profiles on a robotic platform.

With the identification of these gaits families, dynamic climbing robots could choose to change which gait they used based on current attachment conditions. If the surface becomes less reliable for attachment, dynamic walking gaits could be utilized to reduce the chance for detachment. Additionally, by showing the benefits of flight running gaits, while not currently desirable for current dynamic climbing designs, new actuation schemes might be able to overcome the challenges of flight running to enable faster and more efficient running.

References

[1] R. M. Alexander, *Principles of animal locomotion*. Princeton University Press, 2003.

[2] K. Autumn, S. Hsieh, D. Dudek, J. Chen, C. Chitaphan, and R. Full, "Dynamics of geckos running vertically," *Journal of experimental biology*, vol. 209, no. 2, pp. 260–272, 2006.

[3] R. Blickhan, "The spring-mass model for running and hopping," *Journal of Biomechanics*, vol. 22, no. 11-12, pp. 1217–1227, Jan. 1989.

[4] G. A. Cavagna, N. C. Heglund, and C. R. Taylor, "Mechanical work in terrestrial locomotion: two basic mechanisms for minimizing energy expenditure," *American Journal of Physiology-Regulatory, Integrative and Comparative Physiology*, vol. 233, no. 5, pp. R243–R261, 1977.

[5] J. Clark and D. Koditschek, "A spring assisted one degree of freedom climbing model," in *Fast Motions in Biomechanics and Robotics*. Springer Berlin Heidelberg, 2006, pp. 43–64.

[6] S. Collins, A. Ruina, R. Tedrake, and M. Wisse, "Efficient bipedal robots based on passive-dynamic walkers," *Science*, vol. 307, no. 5712, pp. 1082–1085, 2005.

[7] B. Dadashzadeh, H. R. Vejdani, and J. Hurst, "From template to anchor: A novel control strategy for spring-mass running of bipedal robots," in *Intelligent Robots and Systems (IROS 2014), 2014 IEEE/RSJ International Conference on*, Sep. 2014, pp. 2566–2571.

[8] J. Dickson and J. Clark, "The effect of sprawl angle and wall inclination on a bipedal, dynamic climbing platform," in *International Conference on Climbing and Walking Robots and the Support Technologies for Mobile Machines (CLAWAR)*, 2012, pp. 459–66.

[9] R. J. Full and M. S. Tu, "Mechanics of a rapid running insect: two-, four-and six-legged locomotion," *Journal of Experimental Biology*, vol. 156, no. 1, pp. 215–231, 1991.

[10] M. Garcia, A. Chatterjee, A. Ruina, and M. Coleman, "The simplest walking model: stability, complexity, and scaling," *Journal of biomechanical engineering*, vol. 120, no. 2, pp. 281–288, 1998.

[11] H. Geyer, A. Seyfarth, and R. Blickhan, "Compliant leg behaviour explains basic dynamics of walking and running," *Proceedings of the Royal Society of London B: Biological Sciences*, vol. 273, no. 1603, pp. 2861–2867, 2006.

[12] D. I. Goldman, T. S. Chen, D. M. Dudek, and R. J. Full, "Dynamics of rapid vertical climbing in cockroaches reveals a template," *Journal of Experimental Biology*, vol. 209, no. 15, pp. 2990–3000, 2006.

[13] S. Kim, A. T. Asbeck, M. R. Cutkosky, and W. R. Provancher, "Spinybotii: climbing hard walls with compliant microspines," in *Advanced Robotics, 2005. ICAR'05. Proceedings., 12th International Conference on*. IEEE, 2005, pp. 601–606.

[14] S. Kim, M. Spenko, S. Trujillo, B. Heyneman, D. Santos, and M. R. Cutkosky, "Smooth vertical surface climbing with directional adhesion," *Robotics, IEEE Transactions on*, vol. 24, no. 1, pp. 65–74, 2008.

[15] T. L. Lam and Y. Xu, "Climbing strategy for a flexible tree climbing robottreebot," *Robotics, IEEE Transactions on*, vol. 27, no. 6, pp. 1107–1117, 2011.

[16] G. A. Lynch, J. E. Clark, P.-C. Lin, and D. E. Koditschek, "A bioinspired dynamical vertical climbing robot," *The International Journal of Robotics Research*, vol. 31, pp. 974–996, Apr. 2012.

[17] T. McGeer, "Passive dynamic walking," *The international journal of robotics research*, vol. 9, no. 2, pp. 62–82, 1990.

[18] T. A. McMahon, G. Valiant, and E. C. Frederick, "Groucho running," *Journal of Applied Physiology*, vol. 62, no. 6, pp. 2326–2337, 1987.

[19] B. D. Miller and J. E. Clark, "Towards highly-tuned mobility in multiple domains with a dynamical legged platform," *Bioinspiration & biomimetics*, vol. 10, no. 4, p. 046001, 2015.

[20] S. Mochon and T. A. McMahon, "Ballistic walking," *Journal of biomechanics*, vol. 13, no. 1, pp. 49–57, 1980.

[21] M. Raibert, M. Chepponis, and H. Brown, "Running on four legs as though they were one," *IEEE Journal on Robotics and Automation*, vol. 2, no. 2, pp. 70–82, Jun 1986.

[22] Y. Sakagami, R. Watanabe, C. Aoyama, S. Matsunaga, N. Higaki, and K. Fujimura, "The intelligent asimo: System overview and integration," in *Intelligent Robots and Systems, 2002. IEEE/RSJ International Conference on*, vol. 3. IEEE, 2002, pp. 2478–2483.

[23] U. Saranli, M. Buehler, and D. E. Koditschek, "Rhex: A simple and highly mobile hexapod robot," *The International Journal of Robotics Research*, vol. 20, no. 7, pp. 616–631, Jul. 2001.

[24] M. Spenko, G. C. Haynes, J. Saunders, M. R. Cutkosky, A. A. Rizzi, R. J. Full, and D. E. Koditschek, "Biologically inspired climbing with a hexapedal robot," *Journal of Field Robotics*, vol. 25, no. 4-5, pp. 223–242, 2008.